Hindawi Publishing Corporation
Advances in High Energy Physics
Volume 2015, Article ID 593898, 9 pages
http://dx.doi.org/10.1155/2015/593898

Research Article

Z' Resonance and Associated Zh Production at Future Higgs Boson Factory: ILC and CLIC

A. Gutiérrez-Rodríguez[1] and M. A. Hernández-Ruíz[2]

[1] *Facultad de Física, Universidad Autónoma de Zacatecas Apartado Postal C-580, 98060 Zacatecas, ZAC, Mexico*
[2] *Unidad Académica de Ciencias Químicas, Universidad Autónoma de Zacatecas, Apartado Postal C-585, 98060 Zacatecas, ZAC, Mexico*

Correspondence should be addressed to A. Gutiérrez-Rodríguez; alexgu@fisica.uaz.edu.mx

Received 21 April 2015; Revised 23 June 2015; Accepted 24 June 2015

Academic Editor: Sally Seidel

We study the prospects of the $B-L$ model with an additional Z' boson to be a Higgs boson factory at high-energy and high-luminosity linear electron positron colliders, such as the ILC and CLIC, through the Higgs-strahlung process $e^+e^- \rightarrow (Z, Z') \rightarrow Zh$, including both the resonant and the nonresonant effects. We evaluate the total cross section of Zh and we calculate the total number of events for integrated luminosities of 500–2000 fb^{-1} and center of mass energies between 500 and 3000 GeV. We find that the total number of expected Zh events can reach 10^6, which is a very optimistic scenario and it would be possible to perform precision measurements for both Z' and Higgs boson in future high-energy e^+e^- colliders experiments.

1. Introduction

The discovery of a light scalar boson H of the ATLAS [1] and CMS [2] collaborations at the Large Hadron Collider (LHC) compatible with a SM Higgs boson [3–7] and with mass around $M_h = 125 \pm 0.4$ (stat.) $\pm$ 0.5 (syst.) GeV has opened a window to new sectors in the search for physics beyond the Standard Model (SM). The Higgs boson might be a portal leading to more profound physics models and even physics principles. Therefore, another Higgs factory besides the LHC such as the International Linear Collider (ILC) [8–13] and the Compact Linear Collider (CLIC) [14–16] that can study in detail and can precisely determine the properties of the Higgs boson is another important future step in high-energy and high-luminosity physics exploration.

The existence of a heavy neutral (Z') vector boson is a feature of many extensions of the Standard Model. In particular, one (or more) additional $U(1)'$ gauge group provides one of the simplest extensions of the SM. Additional Z' gauge bosons appear in Grand Unified Theories (GUTs) [17], Superstring Theories [18], Left-Right Symmetric Models (LRSM) [19–21], and other models such as models of composite gauge bosons [22]. In particular, it is possible to study some phenomenological features associated with this extra neutral gauge boson by considering a $B-L$ (baryon number minus lepton number) model.

The $B-L$ symmetry plays an important role in various physics scenarios beyond the SM. (a) The gauge $U(1)_{B-L}$ symmetry group is contained in a GUT described by a $SO(10)$ group [23]. (b) The scale of the $B-L$ symmetry breaking is related to the mass scale of the heavy right-handed Majorana neutrinos mass terms providing the well-known see-saw mechanism [24] to explain light left-handed neutrino mass. (c) The $B-L$ symmetry and the scale of its breaking are tightly connected to the baryogenesis mechanism through leptogenesis [25].

The $B-L$ model [26, 27] is attractive due to its relatively simple theoretical structure, and the crucial test of the model is the detection of the new heavy neutral (Z') gauge boson. The analysis of precision electroweak measurements indicates that the new Z' gauge boson should be heavier than about 1.2 TeV [28]. On the other hand, recent bounds from the LHC indicate that the Z' gauge boson should be heavier than about 2 TeV [29, 30], while future LHC runs at 13-14 TeV could increase the Z' mass bounds to higher values or may be lucky and find evidence for its presence. Further studies of the Z' properties will require a new linear collider [31], which will also allow us to perform precision studies of the Higgs sector. Detailed discussions on the $B-L$ model can be found in the literature [26, 32–38].

The Higgs-stralung [39–43] process $e^+e^- \rightarrow Zh$ is one of the main production mechanisms of the Higgs boson in the future linear e^+e^- colliders experiments, such as the ILC and CLIC. Therefore, after the discovery of the Higgs boson, detailed experimental and theoretical studies are necessary for checking its properties and dynamics [44–47]. It is possible to search for the Higgs boson in the framework of the $B-L$ model; however the existence of a new gauge boson could also provide new Higgs particle production mechanisms, which could prove its nonstandard origin. In this work, we analyze how the Z' gauge boson of the $U(1)_{B-L}$ model could be used as a factory of Higgs bosons.

Our aim in the present paper is to study the sensitivity of the Z' boson of the $B-L$ model as a Higgs boson factory through the Higgs-strahlung process $e^+e^- \rightarrow (Z, Z') \rightarrow Zh$, including both the resonant and the nonresonant effects at future high-energy and high-luminosity linear e^+e^- colliders, such as the International Linear Collider (ILC) [8] and the Compact Linear Collider (CLIC) [14]. We evaluate the total cross section of Zh and we calculate the total number of events for integrated luminosities of 500–2000 fb^{-1} and center-of-mass energies between 500 and 3000 GeV. We find that the total number of expected Zh events for the e^+e^- colliders is very promising and that it would be possible to perform precision measurements for both the Z' and the Higgs boson in the future high-energy e^+e^- colliders experiments. In addition, we also studied the dependence of the Higgs signal strengths (μ) on the parameters g_1' and θ_{B-L} of the $U(1)_{B-L}$ model for the Higgs-stralung process $e^+e^- \rightarrow Zh$.

This paper is organized as follows. In Section 2, we present the theoretical framework. In Section 3, we present the decay widths of the Z' boson in the context of the $B-L$ model. In Section 4, we present the calculation of the process $e^+e^- \rightarrow (Z, Z') \rightarrow Zh$, and, finally, we present our results and conclusions in Section 5.

2. Theoretical Framework

We consider an $SU(2)_L \times U(1)_Y \times U(1)_{B-L}$ model consisting of one doublet Φ and one singlet χ and briefly describe the lagrangian including the scalar, fermion, and gauge sector. The Lagrangian for the gauge sector is given by [36, 48–50]

$$\mathscr{L}_g = -\frac{1}{4}B_{\mu\nu}B^{\mu\nu} - \frac{1}{4}W^a_{\mu\nu}W^{a\mu\nu} - \frac{1}{4}Z'_{\mu\nu}Z'^{\mu\nu}, \tag{1}$$

where $W^a_{\mu\nu}$, $B_{\mu\nu}$, and $Z'_{\mu\nu}$ are the field strength tensors for $SU(2)_L$, $U(1)_Y$, and $U(1)_{B-L}$, respectively.

The Lagrangian for the scalar sector of the $SU(2)_L \times U(1)_Y \times U(1)_{B-L}$ model is

$$\mathscr{L}_s = (D^\mu\Phi)^\dagger (D_\mu\Phi) + (D^\mu\chi)^\dagger (D_\mu\chi) - V(\Phi, \chi), \tag{2}$$

where the potential term is [34]

$$\begin{aligned} V(\Phi, \chi) = {} & m^2 (\Phi^\dagger\Phi) + \mu^2 |\chi|^2 + \lambda_1 (\Phi^\dagger\Phi)^2 + \lambda_2 |\chi|^4 \\ & + \lambda_3 (\Phi^\dagger\Phi) |\chi|^2, \end{aligned} \tag{3}$$

with Φ and χ as the complex scalar Higgs doublet and singlet fields, respectively. The covariant derivatives for the doublet and singlet are given by [32–34]

$$\begin{aligned} D^\mu\Phi &= \partial_\mu\Phi + i\left[gT^aW^a_\mu + g_1YB_\mu + g_1'Y'B'_\mu\right]\Phi, \\ D^\mu\chi &= \partial_\mu\chi + i\left[g_1YB_\mu + g_1'Y'B'_\mu\right]\chi, \end{aligned} \tag{4}$$

where the doublet and singlet scalars are

$$\begin{aligned} \Phi &= \begin{pmatrix} G^\pm \\ \dfrac{v + \phi^0 + iG_Z}{\sqrt{2}} \end{pmatrix}, \\ \chi &= \left(\frac{v' + \phi'^0 + iz'}{\sqrt{2}}\right), \end{aligned} \tag{5}$$

with $G^\pm$, G_Z, and z' being the Goldstone bosons of $W^\pm$, Z, and Z', respectively.

After spontaneous symmetry breaking the two scalar fields can be written as

$$\begin{aligned} \Phi &= \begin{pmatrix} 0 \\ \dfrac{v + \phi^0}{\sqrt{2}} \end{pmatrix}, \\ \chi &= \frac{v' + \phi'^0}{\sqrt{2}}, \end{aligned} \tag{6}$$

with v and v' being real and positive. Minimization of (3) gives

$$\begin{aligned} m^2 + 2\lambda_1 v^2 + \lambda_3 v v'^2 &= 0, \\ \mu^2 + 4\lambda_2 v'^2 + \lambda_3 v^2 v' &= 0. \end{aligned} \tag{7}$$

To compute the scalar masses, we must expand the potential in (3) around the minima in (6). Using the minimization conditions, we have the following scalar mass matrix:

$$\mathscr{M} = \begin{pmatrix} \lambda_1 v^2 & \dfrac{\lambda_3 v v'}{2} \\ \dfrac{\lambda_3 v v'}{2} & \lambda_2 v'^2 \end{pmatrix} = \begin{pmatrix} \mathscr{M}_{11} & \mathscr{M}_{12} \\ \mathscr{M}_{21} & \mathscr{M}_{22} \end{pmatrix}. \tag{8}$$

The expressions for the scalar mass eigenvalues ($m_{H'} > m_h$) are

$$m^2_{H',h} = \frac{(\mathscr{M}_{11} + \mathscr{M}_{22}) \pm \sqrt{(\mathscr{M}_{11} - \mathscr{M}_{22})^2 + 4\mathscr{M}^2_{12}}}{2}, \tag{9}$$

and the mass eigenstates are linear combinations of ϕ^0 and ϕ'^0 and written as

$$\begin{pmatrix} h \\ H' \end{pmatrix} = \begin{pmatrix} \cos\alpha & -\sin\alpha \\ \sin\alpha & \cos\alpha \end{pmatrix} \begin{pmatrix} \phi^0 \\ \phi'^0 \end{pmatrix}, \tag{10}$$

where h is the SM-like Higgs boson. The scalar mixing angle α can be expressed as

$$\tan(2\alpha) = \frac{2\mathscr{M}_{12}}{\mathscr{M}_{11} - \mathscr{M}_{22}} = \frac{\lambda_3 v v'}{\lambda_1 v^2 - \lambda_2 v'^2}. \tag{11}$$

In the Lagrangian of the $SU(2)_L \times U(1)_Y \times U(1)_{B-L}$ model, the terms for the interactions between neutral gauge bosons Z, Z' and a pair of fermions of the SM can be written in the form [36, 37]

$$\begin{aligned} \mathscr{L}_{NC} = {} & \frac{-ig}{\cos\theta_W} \sum_f \bar{f} \gamma^\mu \frac{1}{2} \left(g_V^f - g_A^f \gamma^5 \right) f Z_\mu \\ & + \frac{-ig}{\cos\theta_W} \sum_f \bar{f} \gamma^\mu \frac{1}{2} \left(g_V'^f - g_A'^f \gamma^5 \right) f Z'_\mu. \end{aligned} \tag{12}$$

From this Lagrangian we determine the expressions for the new couplings of the Z, Z' bosons with the SM fermions, which are given by

$$\begin{aligned} g_V^f = {} & T_3^f \cos\theta_{B-L} - 2Q_f \sin^2\theta_W \cos\theta_{B-L} \\ & + \frac{2g_1'}{g} \cos\theta_W \sin\theta_{B-L}, \end{aligned} \tag{13}$$

$$\begin{aligned} g_A^f = {} & T_3^f \cos\theta_{B-L}, \\ g_V'^f = {} & -T_3^f \sin\theta_{B-L} - 2Q_f \sin^2\theta_W \sin\theta_{B-L} \\ & + \frac{2g_1'}{g} \cos\theta_W \cos\theta_{B-L}, \\ g_A'^f = {} & -T_3^f \sin\theta_{B-L}, \end{aligned} \tag{14}$$

where $g = e/\sin\theta_W$ and θ_{B-L} is the $Z - Z'$ mixing angle. The current bound on this parameter is $|\theta_{B-L}| \leq 10^{-3}$ [51]. In the decoupling limit, that is to say, when $g_1' = 0$ and $\theta_{B-L} = 0$, the couplings of the SM are recovered.

3. The Decay Widths of Z' in the $B - L$ Model

In this section we present the new decay widths of the Z' boson [28, 52–54] in the context of the $B - L$ model which we need in the calculation of the cross section for the process $e^+e^- \to Zh$. The Z' partial decay widths involving vector bosons and the scalar boson are

$$\begin{aligned} \Gamma\left(Z' \longrightarrow W^+W^-\right) = {} & \frac{G_F M_W^2}{24\pi\sqrt{2}} \cos^2\theta_W \sin^2\theta_{B-L} \\ & \cdot M_{Z'} \left(\frac{M_{Z'}}{M_Z}\right)^4 \left(1 - 4\frac{M_W^2}{M_{Z'}^2}\right)^{1/3} \\ & \cdot \left[1 + 20\frac{M_W^2}{M_{Z'}^2} + 12\frac{M_W^4}{M_{Z'}^4}\right], \\ \Gamma\left(Z' \longrightarrow Zh\right) = {} & \frac{G_F M_Z^2 M_{Z'}}{24\pi\sqrt{2}} \sqrt{\lambda} \left[\lambda + 12\frac{M_Z^2}{M_{Z'}^2}\right] \\ & \cdot \left[f\left(\theta_{B-L}\right)\cos\alpha - g\left(\theta_{B-L}\right)\sin\alpha\right]^2, \end{aligned} \tag{15}$$

where

$$\begin{aligned} \lambda\left(1, \frac{M_Z^2}{M_{Z'}^2}, \frac{M_h^2}{M_{Z'}^2}\right) = {} & 1 + \left(\frac{M_Z^2}{M_{Z'}^2}\right)^2 + \left(\frac{M_h^2}{M_{Z'}^2}\right)^2 \\ & - 2\left(\frac{M_Z^2}{M_{Z'}^2}\right) - 2\left(\frac{M_h^2}{M_{Z'}^2}\right) \\ & - 2\left(\frac{M_Z^2}{M_{Z'}^2}\right)\left(\frac{M_h^2}{M_{Z'}^2}\right), \\ f\left(\theta_{B-L}\right) = {} & \left(\frac{4M_Z^2}{v^2} - g_1'^2\right)\sin\left(2\theta_{B-L}\right) \\ & + \left(\frac{4g_1' M_Z}{v}\right)\cos\left(2\theta_{B-L}\right), \\ g\left(\theta_{B-L}\right) = {} & 4g_1'^2\left(\frac{v'}{v}\right)\sin\left(2\theta_{B-L}\right). \end{aligned} \tag{16}$$

The vacuum expectation value v' is taken as $v' = 2$ TeV, while $\alpha = \pi/9$ for the Higgs mixing parameter in correspondence with [1, 2, 48, 55]. In our analysis we take $v = 246$ GeV and constrain the other scale, v', by the lower bounds imposed on the mass of the extra neutral gauge boson Z'. The mass of the Z' and of the heavy neutrinos depends on v' and should be related to it, while the Higgs masses depend on the angle α, the value of which is completely arbitrary.

Finally, the decay width of the Z' boson to fermions is given by

$$\begin{aligned} \Gamma\left(Z' \longrightarrow f\bar{f}\right) = {} & \frac{2G_F}{3\pi\sqrt{2}} \\ & \cdot N_f M_Z^2 M_{Z'} \sqrt{1 - 4\left(\frac{M_f^2}{M_{Z'}^2}\right)} \left[\left(g_V'^f\right)^2\right. \\ & \left. \cdot \left\{1 + 2\left(\frac{M_f^2}{M_{Z'}^2}\right)\right\} + \left(g_A'^f\right)^2 \left\{1 - 4\left(\frac{M_f^2}{M_{Z'}^2}\right)\right\}\right], \end{aligned} \tag{17}$$

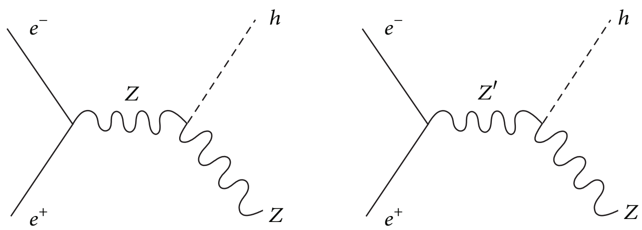

Figure 1: Feynman diagram for the Higgs-strahlung process $e^+e^- \to Zh$ in the $B-L$ model.

where N_f is the color factor ($N_f = 1$ for leptons, $N_f = 3$ for quarks) and the couplings $g_V^{\prime f}$ and $g_A^{\prime f}$ of the Z' boson with the SM fermions are given in (14).

4. The Total Cross Section of $e^+e^- \to Zh$ in the $B-L$ Model

In this section, we calculate the Higgs production cross section via the process $e^+e^- \to Zh$ in the context of the $B-L$ model at future high-energy and high-luminosity linear electron-positron colliders, such as the ILC and CLIC.

The Feynman diagrams contributing to the process $e^+e^- \to (Z, Z') \to Zh$ are shown in Figure 1. The expressions for the total cross section of the Higgs-strahlung process for the different contributions, that is to say SM, $B-L$, and SM $-(B-L)$, respectively, can be written in the following compact form:

$$\begin{aligned}
\sigma\left(e^+e^- \longrightarrow Zh\right)_{\text{tot}} &= \frac{G_F^2 M_Z^4}{24\pi}\left[\left(g_V^e\right)^2 + \left(g_A^e\right)^2\right] \\
&\cdot \frac{s\sqrt{\lambda}\left[\lambda + 12M_Z^2/s\right]}{\left[\left(s-M_Z^2\right)^2 + M_Z^2\Gamma_Z^2\right]} + \frac{G_F^2 M_Z^6}{384\pi}\left[\left(g_V^{\prime e}\right)^2 + \left(g_A^{\prime e}\right)^2\right] \\
&\cdot \frac{s\sqrt{\lambda}\left[\lambda + 12M_{Z'}^2/s\right]}{M_{Z'}^2\left[\left(s-M_{Z'}^2\right)^2 + M_{Z'}^2\Gamma_{Z'}^2\right]}\left[f\left(\theta_{B-L}\right)\cos\alpha - g\left(\theta_{B-L}\right)\right. \\
&\left.\cdot \sin\alpha\right]^2 + \frac{G_F^2 M_Z^6}{12\pi}\left[g_V^e g_V^{\prime e} + g_A^e g_A^{\prime e}\right] \\
&\cdot s\sqrt{\lambda}\left[\frac{1}{M_Z^2}\left(\lambda + 12M_Z^2/s\right)\right. \\
&+ \frac{1}{M_{Z'}^2}\left(\lambda + 6\left(M_Z^2 - M_{Z'}^2\right)/s\right) \\
&\left.+ \frac{s\lambda}{8M_Z^2 M_{Z'}^2}\left(\lambda - 12M_Z^2/s\right)\right] \\
&\cdot \frac{\left[\left(s-M_Z^2\right)\left(s-M_{Z'}^2\right) + M_Z M_{Z'}\Gamma_Z\Gamma_{Z'}\right]}{\left[\left(s-M_Z^2\right)^2 + M_Z^2\Gamma_Z^2\right]\left[\left(s-M_{Z'}^2\right)^2 + M_{Z'}^2\Gamma_{Z'}^2\right]}\left[f\left(\theta_{B-L}\right)\right. \\
&\left.\cdot \cos\alpha - g\left(\theta_{B-L}\right)\sin\alpha\right],
\end{aligned} \tag{18}$$

where

$$\lambda\left(1, \frac{M_Z^2}{s}, \frac{M_h^2}{s}\right) = \left(1 - \frac{M_Z^2}{s} - \frac{M_h^2}{s}\right)^2 - 4\frac{M_Z^2 M_h^2}{s^2} \tag{19}$$

is the usual two-particle phase space function, while g_V^e, g_A^e, $g_V^{\prime e}$, $g_A^{\prime e}$, $f(\theta_{B-L})$, and $g(\theta_{B-L})$ are given in (13), (14), and (16), respectively.

The expression given in the first term of (18) corresponds to the cross section with the exchange of the Z boson, while the second and third terms come from the contributions of the $B-L$ model and of the interference, respectively. The SM expression for the cross section of the reaction $e^+e^- \to Zh$ can be obtained in the decoupling limit, that is to say, when $\theta_{B-L} = 0$ and $g_1' = 0$; in this case the terms that depend on θ_{B-L} and g_1' in (18) are zero and (18) is reduced to the expression given in [39, 43] for the standard model.

5. Results and Conclusions

5.1. Z' Resonance and Associated Zh Production in the $B-L$ Model. In this section we evaluate the total cross section of the Higgs-strahlung process $e^+e^- \to (Z, Z') \to Zh$ in the context of the $B-L$ model at next generation linear e^+e^- colliders such as the ILC and CLIC. Using the following values for numerical computation [51], $\sin^2\theta_W = 0.23126 \pm 0.00022$, $m_\tau = 1776.82 \pm 0.16$ MeV, $m_b = 4.6 \pm 0.18$ GeV, $m_t = 172 \pm 0.9$ GeV, $M_W = 80.389 \pm 0.023$ GeV, $M_Z = 91.1876 \pm 0.0021$ GeV, $\Gamma_Z = 2.4952 \pm 0.0023$ GeV, and $M_h = 125 \pm 0.4$, and considering the most recent limit from LEP [56]

$$\frac{M_{Z'}}{g_1'} \geq 7 \text{ TeV}, \tag{20}$$

in our numerical analysis, we obtain the total cross section $\sigma_{\text{tot}} = \sigma_{\text{tot}}(\sqrt{s}, M_{Z'}, g_1')$. Thus, in our numerical computation, we will assume $\sqrt{s}$, $M_{Z'}$ and g_1' as free parameters.

We do not consider the process $e^+e^- \to (Z, Z') \to ZH'$ [35] in our study since in major parts of the $U(1)_{B-L}$ model parameter space the Higgs boson H' is quite heavy, and it is difficult to detect the process $e^+e^- \to ZH'$ when the relevant mechanism is $e^+e^- \to Zh$.

In Figures 2 and 3 we present the total decay width of the Z' boson as a function of $M_{Z'}$ and the new $U(1)_{B-L}$ gauge coupling g_1', respectively, with the other parameters held fixed to three different values. From Figure 2, we see that the total width of the Z' new gauge boson varies from a few to hundreds of GeV over a mass range of 500 GeV $\leq M_{Z'} \leq$ 3000 GeV, depending on the value of g_1'. In the case of Figure 3, a similar behavior is obtained in the range $0 \leq g_1' \leq 1$ and depends on the value of $M_{Z'}$. The branching ratios versus Z' mass are given in Figure 4 for different channels, that is to say, $\text{BR}(Z' \to f\bar{f})$, $\text{BR}(Z' \to Zh)$, and $\text{BR}(Z' \to W^+W^-)$, respectively. In this figure the $\text{BR}(Z' \to f\bar{f})$ is the sum of all BRs for the decays into fermions. We consider $\theta_{B-L} = 10^{-3}$, $g_1' = 0.5$, and 500 GeV $\leq M_{Z'} \leq$ 3000 GeV.

To illustrate our results on the sensitivity of the Z' gauge boson of the $B-L$ model as a Higgs boson factory through the Higgs-strahlung process $e^+e^- \to (Z, Z') \to Zh$, including both the resonant and the nonresonant effects at future high-energy and high-luminosity linear e^+e^- colliders, such as the International Linear Collider (ILC) and the Compact Linear Collider (CLIC), we present the total cross section in Figures 5–11.

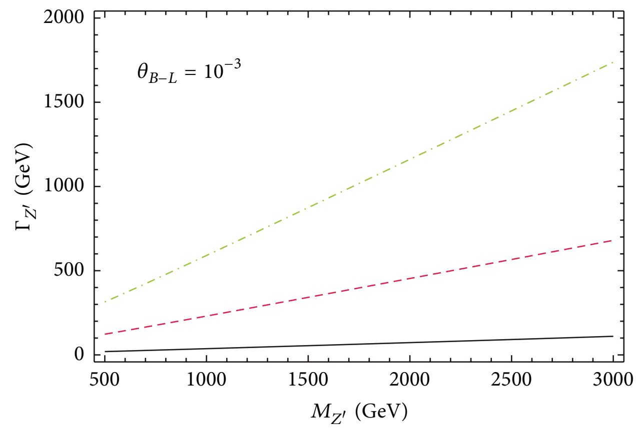

FIGURE 2: Z' width as a function of $M_{Z'}$ for fixed values of g_1'. Starting from the bottom, the curves are for $g_1' = 0.2, 0.5, 0.8$, respectively.

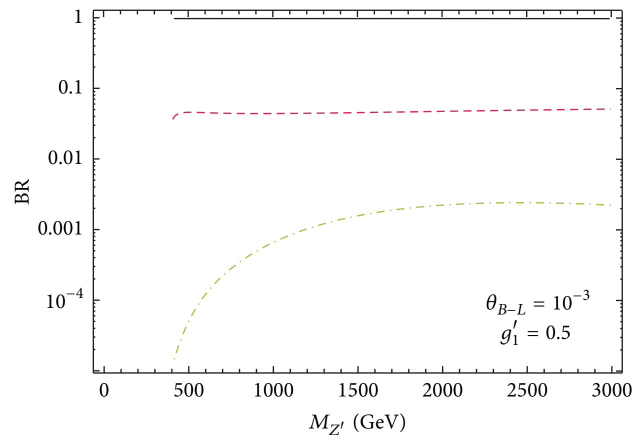

FIGURE 4: Branching ratios as a function of $M_{Z'}$. Starting from the top, the curves are for the BR($f\bar{f}$), BR(Zh), and BR(W^+W^-), respectively.

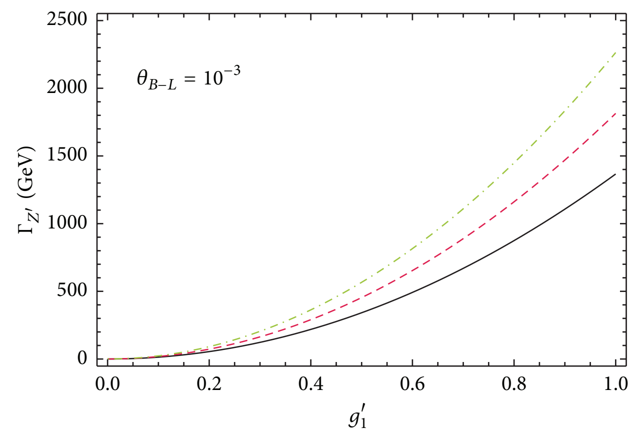

FIGURE 3: Z' width as a function of g_1' for fixed values of $M_{Z'}$. Starting from the bottom, the curves are for $M_{Z'} = 1500, 2000, 2500$ GeV, respectively.

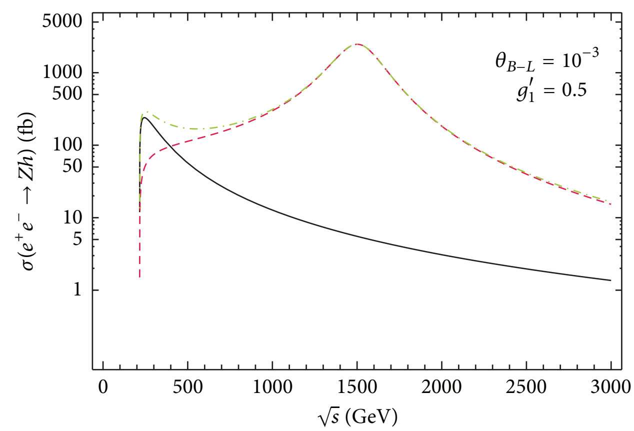

FIGURE 5: The total cross sections of the production processes $e^+e^- \to Zh$ as a function of the collision energy for $M_{Z'} = 1500$ GeV and $M_h = 125$ GeV. The curves are for the first term of (18) (solid line) and second term of (18) (dashed line) and the dot-dashed line corresponds to the total cross section of the process $\sigma(e^+e^- \to Zh)$, respectively.

In Figure 5, we show the cross section $\sigma(e^+e^- \to Zh)$ for the different contributions as a function of the center-of-mass energy $\sqrt{s}$ for $\theta_{B-L} = 10^{-3}$ and $g_1' = 0.5$: the solid line corresponds to the first term of (18), where in the $U(1)_{B-L}$ model the couplings g_V^f and g_A^f of the SM gauge boson Z to electrons receive contributions of the $U(1)_{B-L}$ model. The dashed line corresponds to the second term of (18), that is to say, is the pure $B-L$ contribution. Finally, the dot-dashed line corresponds to the total cross section of the process $\sigma(e^+e^- \to Zh)$. From Figure 5, we can see that the cross section corresponding to the first term of (18) decreases for large $\sqrt{s}$, whereas, in the case of the cross section of the $B-L$ model and the total cross section, respectively, these are increased for large values of the center-of-mass energy, reaching its maximum value at the resonance Z' boson; that is to say, $\sqrt{s} = 1500$ GeV.

To see the effects of g_1', the free parameter of the $B-L$ model on the process $e^+e^- \to (Z, Z') \to Zh$, we plot the relative correction $\delta\sigma/\sigma_{SM} = (\sigma_{tot} - \sigma_{SM})/\sigma_{SM}$ as a function of g_1' for $M_{Z'} = 1500, 2000, 2500$ GeV and $\sqrt{s} = 1500, 2000, 2500$ GeV in Figure 6. We can see that the relative correction reaches its maximum value between $0.1 \leq g_1' \leq 2.5$ and remains almost constant as g_1' increases.

The deviation of the cross section in our model from the SM one $\delta\sigma/\sigma_{SM}$ is depicted in Figure 7 as a function of $M_{Z'}$ for $\sqrt{s} = 1500$ GeV and three values of the g_1', new gauge coupling. Figure 7 shows that the relative correction is very sensitive to the gauge boson mass $M_{Z'}$ and for the gauge parameter $g_1' = 0.2, 0.5, 0.8$ the peak of the total cross section emerges when the heavy gauge boson mass approximately equals $M_{Z'} = 1500, 1450, 1300$ GeV, respectively. Thus, in a sizeable parameter region of the $B-L$ model, the new heavy gauge boson Z' can produce a significant signal, which can be detected in future ILC and CLIC experiments.

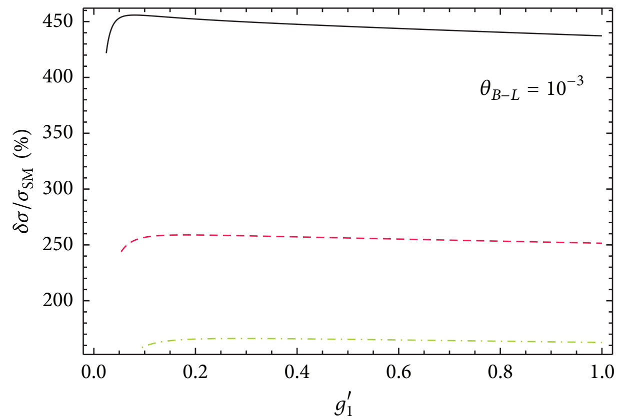

FIGURE 6: The relative correction $\delta\sigma/\sigma_{SM}$ as a function of g_1'. Starting from the top, the curves are for $M_{Z'} = 1500, 2000, 2500$ GeV and $\sqrt{s} = 1500, 2000, 2500$ GeV, respectively.

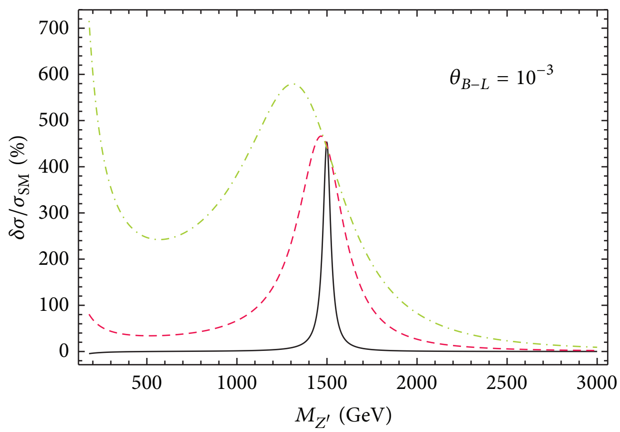

FIGURE 7: The relative correction $\delta\sigma/\sigma_{SM}$ as a function of $M_{Z'}$. Starting from the bottom the curves are for $g_1' = 0.2, 0.5, 0.8$ GeV and $\sqrt{s} = 1500$ GeV, respectively.

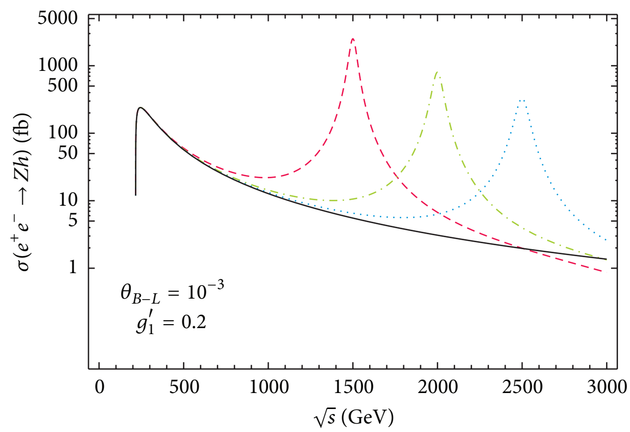

FIGURE 8: The total cross sections of the production processes $e^+e^- \to Zh$ as a function of the collision energy. The curves are for SM (solid line) and $M_{Z'} = 1500, 2000, 2500$ GeV (dashed line, dot-dashed line, and dotted line). The resonance corresponds to the Z' new gauge boson.

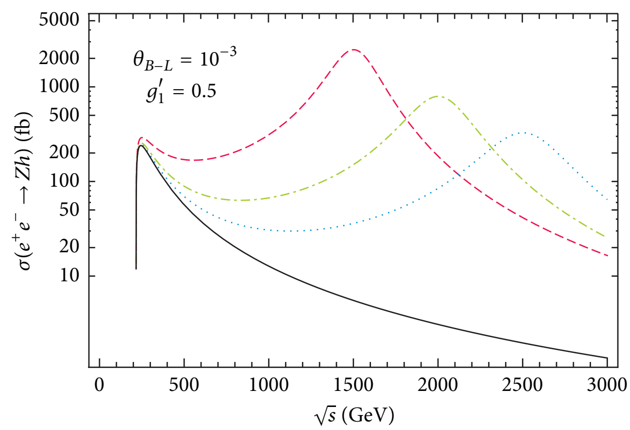

FIGURE 9: The same as Figure 8 but for $g_1' = 0.5$.

We plot the total cross section of the reaction $e^+e^- \to Zh$ in Figure 8 as a function of the center-of-mass energy, $\sqrt{s}$ for the values of the heavy gauge boson mass of $M_{Z'} = 1500, 2000, 2500$ GeV and $\theta_{B-L} = 10^{-3}$, $g_1' = 0.2$, respectively. In this figure we observed that, for $\sqrt{s} = M_{Z'}$, the resonant effect dominates the Higgs particle production. A similar analysis was performed in Figure 9, but in this case $\theta_{B-L} = 10^{-3}$ and $g_1' = 0.5$. In both figures we show that the cross section is sensitive to the free parameters. Comparing Figures 8 and 9, we observe that the height of the resonances is the same in both figures, but the resonances are broader for larger g_1' values, as the total width of the Z' boson increases with g_1', as it is shown in Figure 2.

Finally, in Figure 10 we use the currents values of $M_{Z'}$ and θ_{B-L}, as well as the value of the coupling constant g_1' and center-of-mass energy $\sqrt{s}$ of the collider to obtain contour plot 3D for the total cross section $\sigma_{tot} = \sigma_{tot}(\sqrt{s}, M_{Z'}, g_1')$ of the process $e^+e^- \to Zh$ for $M_h = 125$ GeV and $\theta_{B-L} = 10^{-3}$. In this figure the resonance peaks for the boson Z' are evident for the entire range of allowed parameters of the $U(1)_{B-L}$ model.

From Figures 5–10, it is clear that the total cross section is sensitive to the value of the gauge boson mass $M_{Z'}$, center-of-mass energy $\sqrt{s}$, and g_1'; the new $U(1)_{B-L}$ gauge coupling increases with the collider energy, reaching a maximum at the resonance of the Z' gauge boson. As an indicator of the order of magnitude, we present the Zh number of events in Table 1, for several gauge boson masses, center-of-mass energies, and g_1' values and for a luminosity of $\mathscr{L} = 500, 1000, 2000\ \text{fb}^{-1}$. We find that the possibility of observing the process $e^+e^- \to (Z, Z') \to Zh$ is very promising as shown in Table 1, and it would be possible to perform precision measurements for both the Z' and the Higgs boson in the future high-energy linear e^+e^- colliders experiments. We observed in Table 1 that the cross section rises once the threshold for Zh production is reached, with the energy, until the Z' is produced resonantly at $\sqrt{s} = 1500$, 2000, and 2500 GeV, respectively, for the three cases. Afterwards it decreases with rising energy due to the Z and Z' propagators. Another promising production mode for

TABLE 1: Total production of ZH in the $B-L$ model for $M_{Z'}$ = 1500, 2000, 2500 GeV, $\mathscr{L}$ = 500, 1000, 2000 fb^{-1} (1st, 2nd, and 3rd numbers, respectively, in the last 3 columns), M_H = 125 GeV, g_1' = 0.5, and $\theta_{B-L} = 10^{-3}$.

	$\mathscr{L}$ = 500, 1000, 2000 fb^{-1}		
$\sqrt{s}$	$M_{Z'}$ = 1500 GeV	$M_{Z'}$ = 2000 GeV	$M_{Z'}$ = 2500 GeV
500	85 131; 170 263; 340 526	44 609; 89 219; 178 439	34 747; 69 493; 138 987
1000	155 482; 310 964; 621 928	33 523; 67 047; 134 094	15 339; 30 678; 61 355
1500	1 234 000; 2 460 000; 4 930 000	75 192; 150 384; 300 768	18 004; 36 008; 72 016
2000	92 640; 185 282; 370 564	396 490; 792 980; 1 580 000	42 224; 84 449; 168 899
2500	20 276; 41 534; 83 069	52 144; 104 288; 208 577	163 538; 327 076; 654 151
3000	8 243; 16 487; 32 974	12 721; 25 442; 50 885	32 173; 64 346; 128 693

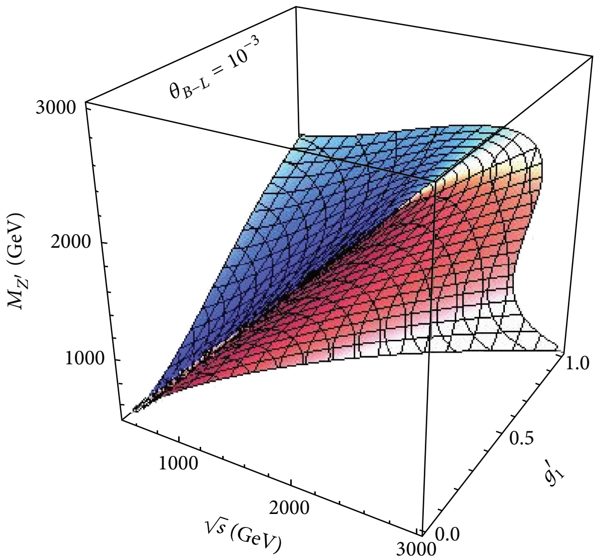

FIGURE 10: Contour plot 3D for the total cross section $\sigma_{\text{tot}} = \sigma_{\text{tot}}(\sqrt{s}, M_{Z'}, g_1')$ of the process $e^+e^- \to Zh$ for M_h = 125 GeV and $\theta_{B-L} = 10^{-3}$.

studying the Z' boson and Higgs boson properties is $e^+e^- \to (\gamma, Z, Z') \to t\bar{t}h$ [57].

5.2. The Higgs Signal Strengths in the B–L Model. Considering the Higgs boson decay channels, the Higgs signal strengths can be defined as

$$\mu_i = \frac{\sigma_{B-L} \times \text{BR}(h \to i)_{B-L}}{\sigma_{\text{SM}} \times \text{BR}(h \to i)_{\text{SM}}}, \tag{21}$$

where i denotes a possible final state of the Higgs boson decay, for example, $b\bar{b}, W^+W^-, ZZ, gg$, and $\gamma\gamma$.

Fixing the Higgs boson mass to the measured value and considering the decays $h \to \gamma\gamma$, $h \to ZZ$, $h \to W^+W^-$, $h \to b\bar{b}$, and $h \to \tau^+\tau^-$, the ATLAS collaboration reports [58] a signal strength of

$$\mu = 1.18^{+0.15}_{-0.14}. \tag{22}$$

The corresponding CMS collaboration result [59] is

$$\mu = 1.00 \pm 0.13. \tag{23}$$

Good consistency is found, for both experiments, across different decay modes and analyses categories related to different production modes.

In the $B-L$ model, the modifications of the $hf\bar{f}$ (the SM fermions pair) and hVV ($V = W, Z$) couplings can give the extra contributions to the Higgs boson production processes. On the other hand, the loop-induced couplings, such as $h\gamma\gamma$ and hgg, could also be affected. Finally, besides the effects already seen in the Higgs-strahlung channel due to the couplings equations (13) and (14) and the functions given by (16), the exchange of s-channel heavy neutral gauge boson Z' also affected the production cross section. All effects can modify the signal strengths in a way that may be detectable at the future ILC/CLIC experiments.

In Figure 11, we show the dependence of the Higgs signal strengths μ_i ($i = b\bar{b}, \gamma\gamma$) on the parameters g_1' and θ_{B-L} for the Higgs-strahlung process $e^+e^- \to (Z, Z') \to Zh$, where (a) and (b) denote the Higgs signal strengths $\mu_{b\bar{b}}$ and $\mu_{\gamma\gamma}$, respectively.

Using $\theta_{B-L} = 10^3$ for the mixing angle and M_h = 125 GeV for the Higgs boson mass, the following bound on the signal strength is obtained:

$$\mu = 1.2^{+0.12}_{-0.16}, \tag{24}$$

which is consistent with that obtained for the ATLAS [58] and CMS [59] collaborations, (22) and (23), respectively.

In conclusion, we consider the Z' heavy gauge boson of the $B-L$ model as a Higgs boson factory, through the Higgs-strahlung process $e^+e^- \to (Z, Z') \to Zh$. We find that the future linear e^+e^- colliders experiments such as the ILC and CLIC could test the $B-L$ model by measuring the cross section of the process $e^+e^- \to Zh$, and it would be possible to perform precision measurements of the Z' gauge boson and of the h Higgs boson, as well as of the parameters of the model θ_{B-L} and g_1', complementing other studies on the $B-L$ model and on the Higgs-strahlung process. The SM expression for the cross section of the reaction $e^+e^- \to Zh$ can be obtained in the decoupling limit; that is to say, when $\theta_{B-L} = 0$ and $g_1' = 0$, in this case the terms that depend on θ_{B-L} and g_1' in (18) are zero and (18) is reduced to the expression given in [39, 43] for the standard model. We also studied the dependence of the Higgs signal strengths (μ) on the parameters g_1' and θ_{B-L} of the $U(1)_{B-L}$ model for the Higgs-stralung process $e^+e^- \to Zh$. We obtain a bound on (μ), which is consistent with that obtained for the ATLAS [58]

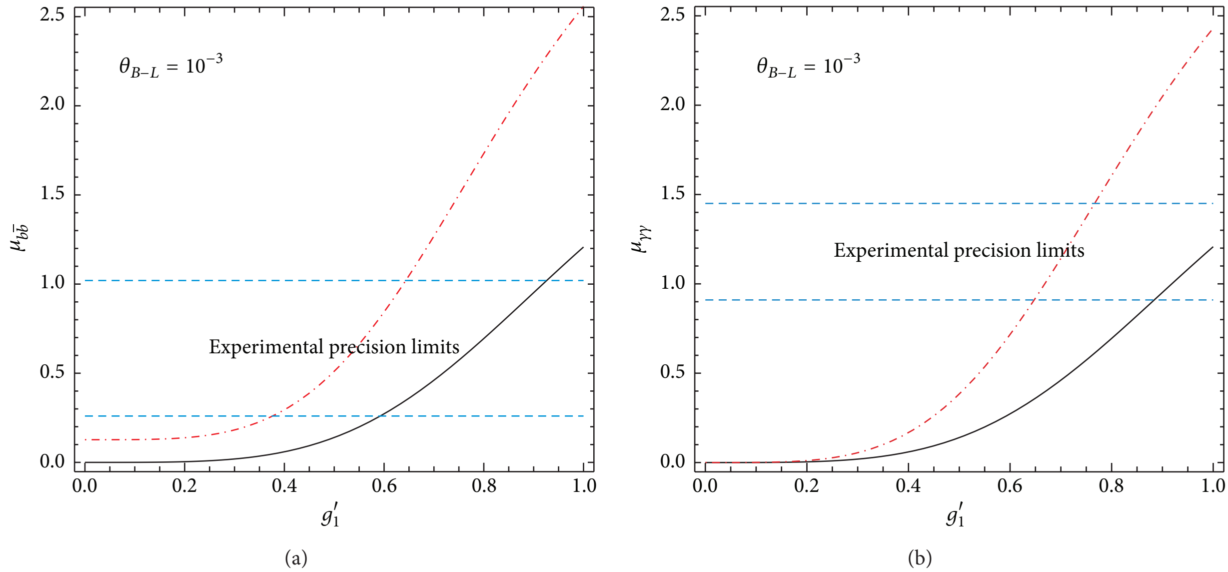

FIGURE 11: Higgs signal strengths μ_i $(i = b\bar{b}, \gamma\gamma)$ for the process $e^+e^- \rightarrow Zh$ as a function of g'_1. The dashed lines represent the experimental precision limits and the solid and dot-dashed lines correspond to the $U(1)_{B-L}$ model with $M_h = 125$ GeV and $\sqrt{s} = 500, 1500$ GeV, respectively.

and CMS [59] collaborations. In addition, the analytical and numerical results for the total cross section have never been reported in the literature before and could be of relevance for the scientific community.

Conflict of Interests

The authors declare that there is no conflict of interests regarding the publication of this paper.

Acknowledgments

The authors acknowledge support from CONACyT, SNI, PROMEP, and PIFI (Mexico).

References

[1] G. Aad, T. Abajyan, B. Abbott et al., "Observation of a new particle in the search for the Standard Model Higgs boson with the ATLAS detector at the LHC," *Physics Letters B*, vol. 716, no. 1, pp. 1–29, 2012.

[2] S. Chatrchyan, V. Khachatryan, A. M. Sirunyan et al., "Observation of a new boson at a mass of 125 GeV with the CMS experiment at the LHC," *Physics Letters B*, vol. 716, no. 1, pp. 30–61, 2012.

[3] P. Higgs, "Broken symmetries, massless particles and gauge fields," *Physics Letters*, vol. 12, no. 2, pp. 132–133, 1964.

[4] P. W. Higgs, "Broken symmetries and the masses of gauge bosons," *Physical Review Letters*, vol. 13, pp. 508–509, 1964.

[5] P. W. Higgs, "Spontaneous symmetry breakdown without massless bosons," *Physical Review*, vol. 145, no. 4, pp. 1156–1163, 1966.

[6] F. Englert and R. Brout, "Broken symmetry and the mass of gauge vector mesons," *Physical Review Letters*, vol. 13, no. 9, article 321, 1964.

[7] G. S. Guralnik, C. R. Hagen, and T. W. B. Kibble, "Global conservation laws and massless particles," *Physical Review Letters*, vol. 13, no. 20, pp. 585–587, 1964.

[8] T. Abe, N. Arkani-Hamed, D. Asner et al., "Linear collider physics resource book for snowmass 2001—part 3: studies of exotic and standard model physics," http://arxiv.org/abs/hep-ex/0106057.

[9] G. Aarons, T. Abe, J. Abernathy et al., "International linear collider reference design report volume 2: physics at the ILC," http://arxiv.org/abs/0709.1893.

[10] J. Brau, Y. Okada, N. Walker et al., "ILC reference design report volume 1—executive summary," http://arxiv.org/abs/0712.1950.

[11] H. Baer, T. Barklow, K. Fujii et al., "The international linear collider technical design report—volume 2: physics," http://arxiv.org/abs/1306.6352.

[12] D. M. Asner, T. Barklow, C. Calancha et al., "ILC higgs white paper," http://arxiv.org/abs/1310.0763.

[13] P. M. Zerwas, Ed., *Proceedings of the Workshop on e^+e^- Collisions at 500 GeV: The Physics Potential, Munich-Annecy-Hamburg, February to September 1991*, Reports DESY 92-123A, B; 93-123C, DESY, 1992.

[14] E. Accomando, A. Aranda, E. Ateser et al., "Physics at the CLIC multi-TeV linear collider," http://arxiv.org/abs/hep-ph/0412251.

[15] D. Dannheim, P. Lebrun, L. Linssen et al., "CLIC e^+e^- linear collider studies," http://arxiv.org/abs/1208.1402.

[16] H. Abramowicz, A. Abusleme, K. Afanaciev et al., "Physics at the CLIC e^+e^- linear collider—input to the Snowmass process 2013," http://arxiv.org/abs/1307.5288.

[17] R. W. Robinett, "Neutral currents in E_6," *Physical Review D*, vol. 26, no. 9, pp. 2388–2395, 1982.

[18] M. B. Green and J. H. Schwarz, "Anomaly cancellations in supersymmetric $D = 10$ gauge theory and superstring theory," *Physics Letters B*, vol. 149, no. 1–3, pp. 117–122, 1984.

[19] R. N. Mohapatra and P. B. Pal, in *Massive Neutrinos in Physics and Astrophysics*, vol. 41 of *Lecture Notes in Physics*, World Scientific, Singapore, 1991.

[20] G. Senjanović, "Spontaneous breakdown of parity in a class of gauge theories," *Nuclear Physics B*, vol. 153, no. 3-4, pp. 334–364, 1979.

[21] G. Senjanovic and R. N. Mohapatra, "Exact left-right symmetry and spontaneous violation of parity," *Physical Review D*, vol. 12, no. 5, pp. 1502–1505, 1975.

[22] U. Baur, D. Schildknecht, and K. H. Schwarzer, "Excited weak vector bosons," *Physical Review D*, vol. 35, p. 297, 1987.

[23] W. Buchmuller, C. Greub, and P. Minkowski, "Neutrino masses, neutral vector bosons and the scale of B–L breaking," *Physics Letters B*, vol. 267, no. 3, pp. 395–399, 1991.

[24] R. N. Mohapatra and G. Senjanović, "Neutrino mass and spontaneous parity nonconservation," *Physical Review Letters*, vol. 44, no. 14, pp. 912–915, 1980.

[25] M. Fukugita and T. Yanagida, *Physics of Neutrinos and Applications to Astrophysics*, Springer, Berlin, Germany, 2003.

[26] L. Basso, A. Belyaev, S. Moretti, and C. H. Shepherd-Themistocleous, "Phenomenology of the minimal B–L extension of the standard model: Z' and neutrinos," *Physical Review D*, vol. 80, no. 5, Article ID 055030, 14 pages, 2009.

[27] L. Basso, A. Belyaev, S. Moretti, and G. M. Pruna, "Probing the Z' sector of the minimal B-L model at future linear colliders in the $e^+e^- \rightarrow \mu^+\mu^-$ process," *Journal of High Energy Physics*, vol. 2009, no. 10, article 006, 2009.

[28] P. Langacker, "The physics of heavy Z' gauge bosons," *Reviews of Modern Physics*, vol. 81, no. 3, pp. 1199–1228, 2009.

[29] ATLAS Collaboration, "Search for high-mass dilepton resonances in 20/fb of pp collisions at $\sqrt{s} = 8$ TeV with the ATLAS experiment," ATLAS-CONF-2013-017, 2013.

[30] CMS Collaboration, "Search for resonances in the dilepton mass distribution in pp collisions at $\sqrt{s} = 8$ TeV," Tech. Rep. CMS-PAS-EXO-12-061, CERN, 2013.

[31] B. C. Allanach, G. A. Blair, S. Kraml et al., "Reconstructing supersymmetric theories by coherent LHC/LC analyses," http://arxiv.org/abs/hep-ph/0403133.

[32] L. Basso, A. Belyaev, S. Moretti, G. M. Pruna, and C. H. Shepherd-Themistocleous, "$Z\prime$ discovery potential at the LHC in the minimal B–L extension of the standard model," *The European Physical Journal C*, vol. 71, article 1613, 2011.

[33] L. Basso, S. Moretti, and G. M. Pruna, "Constraining the ${g'}_1$ coupling in the minimal B-L model," *Journal of Physics G: Nuclear and Particle Physics*, vol. 39, no. 2, Article ID 025004, 2012.

[34] L. Basso, S. Moretti, and G. M. Pruna, "Renormalization group equation study of the scalar sector of the minimal $B - L$ extension of the standard model," *Physical Review D*, vol. 82, Article ID 055018, 2010.

[35] L. Basso, S. Moretti, and G. M. Pruna, "The Higgs sector of the minimal B–L model at future Linear Colliders," *The European Physical Journal C*, vol. 71, article 1724, 2011.

[36] L. Basso, "Phenomenology of the minimal B-L extension of the Standard Model at the LHC," http://arxiv.org/abs/1106.4462.

[37] J. L. Díaz-Cruz, J. M. Hernández-López, and J. A. Orduz-Ducuara, "An extra Z' gauge boson as a source of Higgs particles," *Journal of Physics G: Nuclear and Particle Physics*, vol. 40, no. 12, Article ID 125002, 2013.

[38] S. Iso, N. Okada, and Y. Orikasa, "Minimal B–L model naturally realized at the TeV scale," *Physical Review D*, vol. 80, no. 11, Article ID 115007, 12 pages, 2009.

[39] J. Ellis, M. K. Gaillard, and D. V. Nanopoulos, "A phenomenological profile of the Higgs boson," *Nuclear Physics B*, vol. 106, pp. 292–340, 1976.

[40] B. L. Ioffe and V. A. Khoze, "What can be expected from experiments on colliding e^+e^- beams with e approximately equal to 100-GeV?" *Soviet Journal of Nuclear Physics*, vol. 9, p. 50, 1978.

[41] B. W. Lee, C. Quigg, and H. B. Thacker, "Weak interactions at very high energies: the role of the Higgs-boson mass," *Physical Review D*, vol. 16, no. 5, pp. 1519–1531, 1977.

[42] J. D. Bjorken, "Lectures on the new particles," in *Proceedings of the Summer Institute on Particle Physics*, SLAC Report 198, 1976.

[43] V. D. Barger, K. Cheung, A. Djouadi, B. A. Kniehl, and P. M. Zerwas, "Higgs bosons: intermediate mass range at e^+e^- colliders," *Physical Review D*, vol. 49, no. 1, pp. 79–90, 1994.

[44] J. Ellis, "Higgs physics," http://arxiv.org/abs/1312.5672.

[45] S. Dawson, A. Gritsan, H. Logan et al., "Higgs working group report of the snowmass 2013 community planning study," http://arxiv.org/abs/1310.8361.

[46] M. Klute, R. Lafaye, T. Plehn, M. Rauch, and D. Zerwas, "Measuring Higgs couplings at a linear collider," *Europhysics Letters*, vol. 101, no. 5, Article ID 51001, 2013.

[47] T. Behnke, J. E. Brau, B. Foster et al., "The international linear collider technical design report—volume 1: executive summary," http://arxiv.org/abs/1306.6327.

[48] S. Khalil, "Low-scale B-L extension of the standard model," *Journal of Physics G: Nuclear and Particle Physics*, vol. 35, no. 5, Article ID 055001, 2008.

[49] A. Ferroglia, A. Lorca, and J. J. van der Bij, "The Z' reconsidered," *Annals of Physics*, vol. 16, no. 7-8, pp. 563–578, 2007.

[50] T. G. Rizzo, "Z' phenomenology and the LHC," http://arxiv.org/abs/hep-ph/0610104.

[51] K. A. Olive, K. Agashe, C. Amsler et al., "Review of particle physics," *Chinese Physics C*, vol. 38, no. 39, Article ID 090001, 2014.

[52] A. Leike, "The phenomenology of extra neutral gauge bosons," *Physics Report*, vol. 317, no. 3-4, pp. 143–250, 1999.

[53] R. W. Robinett and J. L. Rosner, "Prospects for a second neutral vector boson at low mass in SO(10)," *Physical Review D*, vol. 25, pp. 3036–3064, 1982.

[54] V. Barger and K. Whisnant, "Heavy-Z-boson decays to two bosons in E_6 superstring models," *Physical Review D*, vol. 36, no. 11, pp. 3429–3437, 1987.

[55] L. Basso, S. Moretti, and G. M. Pruna, "Phenomenology of the minimal $B - L$ extension of the standard model: the Higgs sector," *Physical Review D*, vol. 83, Article ID 055014, 2011.

[56] G. Cacciapaglia, C. Csáki, G. Marandella, and A. Strumia, "The minimal set of electroweak precision parameters," *Physical Review D*, vol. 74, no. 3, Article ID 033011, 2006.

[57] A. Gutiérrez-Rodríguez and M. A. Hernández-Ruíz, Work in progress.

[58] ATLAS Collboration, "Measurements of the Higgs boson production and decay rates and couplings using pp collision data at $\sqrt{s} = 7$ and 8 TeV in the ATLAS experiment," Tech. Rep. ATLAS-CONF-2015-007, 2015.

[59] V. Khachatryan, A. M. Sirunyan, A. Tumasyan et al., "Precise determination of the mass of the Higgs boson and tests of compatibility of its couplings with the standard model predictions using proton collisions at 7 and 8 TeV," *The European Physical Journal C*, vol. 75, article 212, 2015.